NEUROSCIENCE

Multiplex quantitative assays indicate a need for re-evaluating reported small-molecule TrkB agonists

Umed Boltaev,[1,2]* Yves Meyer,[1]* Farangis Tolibzoda,[1,2] Teresa Jacques,[1] Madalee Gassaway,[1,2] Qihong Xu,[3] Florence Wagner,[3] Yan-Ling Zhang,[3] Michelle Palmer,[3] Edward Holson,[3] Dalibor Sames[1,2]†

Brain-derived neurotrophic factor (BDNF) and its receptor, tropomyosin-related kinase B (TrkB), have emerged as key regulators of brain plasticity and represent disease-modifying targets for several brain disorders, including Alzheimer's disease and major depressive disorder. Because of poor pharmacokinetic properties of BDNF, the interest in small-molecule TrkB agonists and modulators is high. Several compounds have been reported to act as TrkB agonists, and their increasing use in various nervous system disorder models creates the perception that these are reliable probes. To examine key pharmacological parameters of these compounds in detail, we have developed and optimized a series of complementary quantitative assays that measure TrkB receptor activation, TrkB-dependent downstream signaling, and gene expression in different cellular contexts. Although BDNF and other neurotrophic factors elicited robust and dose-dependent receptor activation and downstream signaling, we were unable to reproduce these activities using the reported small-molecule TrkB agonists. Our findings indicate that experimental results obtained with these compounds must be carefully interpreted and highlight the challenge of developing reliable pharmacological activators of this key molecular target.

INTRODUCTION

Brain-derived neurotrophic factor (BDNF) and its primary receptor, tropomyosin-related kinase B (TrkB), have emerged as key regulators of neuroplasticity in the development and maintenance of the nervous system. BDNF release and TrkB activation lead to enhanced neurogenesis of different neurochemical cell types, synaptogenesis, and synaptic plasticity (*1*, *2*), all of which affect memory (*3*) and cognitive enhancements (Fig. 1) (*4*, *5*). Augmentation of TrkB signaling, either pharmacologically or through BDNF infusion, induces brain plasticity similar to that observed during the postnatal developmental period, thus enabling circuitry rewiring and recovery of lost function in the context of rodent disease models (*6*).

The potential therapeutic effects of targeting BDNF signaling are widely studied in animal models of brain disorders. BDNF infusion into select brain areas of mice or rats shows antidepressant (*7*–*9*) and anxiolytic effects (*10*, *11*) by inducing synaptic plasticity (*12*, *13*). Similar neuroplasticity effects induced in relevant circuits by antidepressants, such as fluoxetine, are likely required for the therapeutic efficacy of these drugs (*14*). Chronic administration of fluoxetine and other selective serotonin reuptake inhibitors increases the phosphorylation of TrkB in the hippocampus and prefrontal cortex (*15*), and deletion of TrkB in hippocampal neurons of newborn mice inhibits the effects of antidepressants (*16*) and increases anxiety-like behavior in these animals (*17*). Furthermore, one of the mechanistic models for the fast-acting antidepressant effect of ketamine invokes activity-dependent release of BDNF as the required downstream event after ketamine administration (*18*). Collectively, these data indicate that the BDNF-TrkB signaling system is required for the induction of neuroplasticity and subsequent reversal of wiring and functional deficiencies, ultimately resulting in antidepressant activity (*12*).

BDNF has also been pursued as an experimental treatment of neurological and neurodegenerative diseases (*19*, *20*). For example, delivery of BDNF into the striatum has been shown to attenuate the progression of Huntington's disease in animal models (*21*). BDNF concentration was found to be reduced in parietal cortices and hippocampi in postmortem brains of Alzheimer's disease patients (*22*), and another report revealed that amyloid-β peptide induces truncation of TrkB and reduction of TrkB signaling (*23*). Owing to its role in this multitude of brain processes, studies focusing on the BDNF-TrkB signaling pathway are highly represented in the scientific and medical literature, with an exponential increase in the number of publications since 2000 (1700 papers in 2016, through PubMed search) (*24*).

Because the use of BDNF as a biopharmaceutical has been difficult owing to its poor pharmacokinetic properties (*19*, *20*), development of small-molecule TrkB agonists and modulators has become an important goal (*25*). Several small-molecule agonists have been reported to activate TrkB (Fig. 1) in living cells in vitro, including 7,8-dihydroxyflavone (7,8-DHF) (*26*), deoxygedunin (*27*), LM22A-4 (*28*), demethylasterriquinone B1 (DMAQ-B1) (*29*), amitriptyline (*30*), and deprenyl (*31*). DMAQ-B1 was identified by screening a natural product library for activation of the insulin receptor (*32*) and has been reported to also activate TrkA, TrkB, and TrkC (*29*). Deoxygedunin and 7,8-DHF were identified by screening natural product libraries for compounds that protect against staurosporine-induced apoptosis in murine brain–derived cell line overexpressing TrkB (*26*). These studies reported evidence for direct binding of 7,8-DHF to the extracellular domain of TrkB, based on surface plasmon resonance and other biochemical assays, and TrkB phosphorylation by Western blots of rat primary cortical neuron cultures (*33*). Deoxygedunin was shown to promote axonal regeneration (*34*). LM22A-4 was identified through an in silico screening method based on structural analysis of BDNF loop 2, which was assumed to interact with TrkB, and was reported to activate TrkB and downstream targets in mouse hippocampal neuron culture (*28*). In vivo LM22A-4 improved motor and respiratory functions in mouse models of Rett syndrome and Huntington's disease, respectively (*35*, *36*). Amitriptyline has been reported to induce TrkB phosphorylation and neurite outgrowth in vitro

[1]Department of Chemistry, Columbia University, New York, NY 10027, USA. [2]NeuroTechnology Center at Columbia University, New York, NY 10027, USA. [3]Stanley Center for Psychiatric Research, Broad Institute of Massachusetts Institute of Technology and Harvard, 7 Cambridge Center, Cambridge, MA 02142, USA.
*These authors contributed equally to this work.
†Corresponding author. Email: sames@chem.columbia.edu

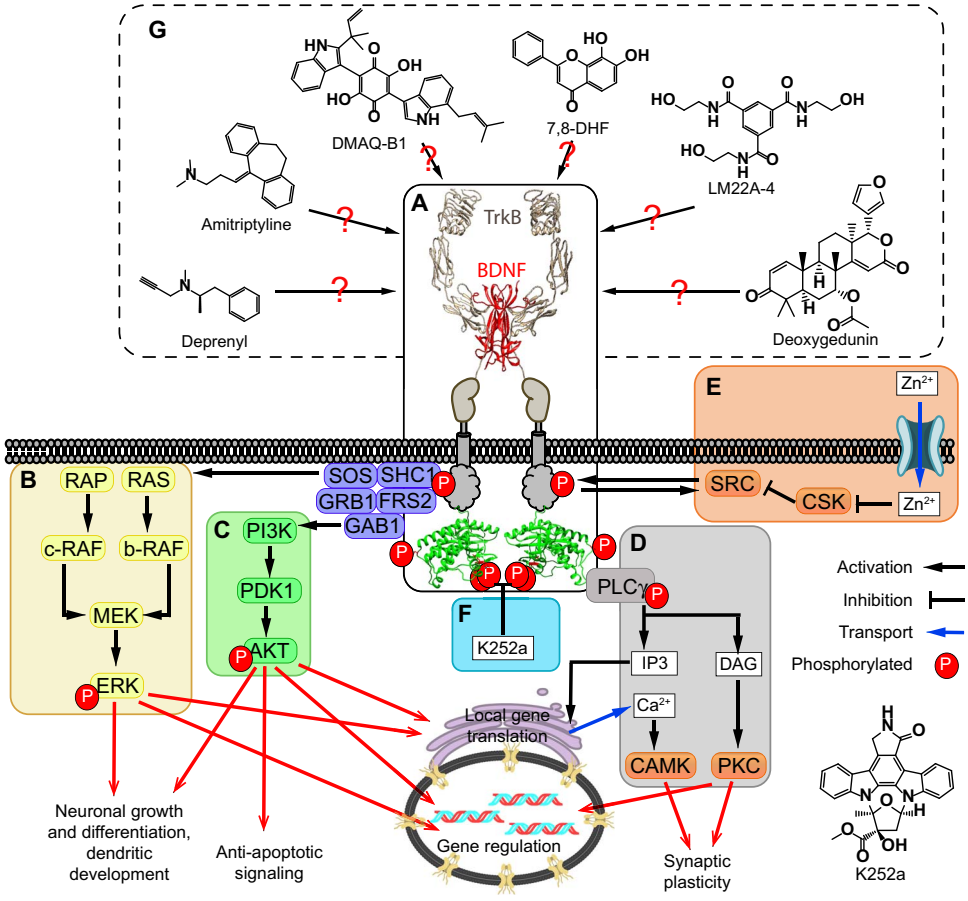

Fig. 1. TrkB signaling and reported small-molecule agonists. (**A**) TrkB contains several domains, including a ligand-binding site in the extracellular portion, a single-transmembrane α helix, a juxtamembrane region, and an intracellular tyrosine kinase domain. Homodimers of BDNF, NT3, or NT4 induce TrkB dimerization and kinase activation through a series of autophosphorylation events at Tyr^{515}, $Tyr^{705–706}$, and Tyr^{816} (*64*). (**B** and **C**) SHC1 and other signaling and adaptor proteins are recruited to TrkB that is phosphorylated at Tyr^{515} ($pTyr^{515}$) and trigger signaling through the RAS-ERK (RAS–extracellular signal–regulated kinase) (B) and PI3K (phosphatidylinositol 3-kinase)–AKT (C) cascades. (**D**) Phosphorylation of TrkB at Tyr^{816} elicits activation of PLCγ (phospholipase C–γ), which triggers PKC (protein kinase C)–Ca^{2+} signaling. These pathways collectively account for anti-apoptotic signaling, local protein synthesis, and gene regulation that ultimately lead to increased neurogenesis, neuronal growth and differentiation, synaptogenesis, synaptic plasticity, and other physiological effects of BDNF and other neurotrophic factors. (**E**) It has been reported that Zn^{2+} transactivates TrkB through an indirect mechanism (*40*) in which Zn^{2+} ions inhibit the kinase CSK (C-terminal SRC kinase), thus preventing it from inhibiting the kinase SRC. Disinhibited SRC then phosphorylates TrkB at $Tyr^{706–707}$, which in turn activates the TrkB kinase domain, leading to phosphorylation of other tyrosine residues required for signaling through the ERK and AKT pathways. SRC and TrkB also mutually activate each other (*42*). (**F**) K252a is a compound that inhibits TrkB by binding to the tyrosine kinase domain (*41*). (**G**) Several small molecules have been reported to activate TrkB by acting as agonists.

RESULTS

Direct measurement of TrkB phosphorylation by quantitative sandwich enzyme-linked immunosorbent assay

Because activation of TrkB is associated with phosphorylation at several tyrosine residues (Fig. 1), we developed a sandwich-style enzyme-linked immunosorbent assay (ELISA) to detect global TrkB tyrosine phosphorylation (fig. S1). ELISA also allowed us to test multiple experimental conditions with several replicates within a single plate, which is typically impractical using Western blotting. To test the dynamic range of the assay, we used it to generate dose-response curves for several neurotrophic factors in rat primary cortical neuron culture (Fig. 2A). Specifically, BDNF [EC_{50} (half maximal effective concentration), 1.1 ± 0.4 nM] was used as the reference for full activation (full agonism), and the amount of TrkB phosphorylation induced by BDNF was defined as 100%. Neurotrophin-4 (NT4; EC_{50}, 1.2 ± 0.4 nM) was a high-efficacy agonist in this assay, exhibiting 73 ± 6% efficacy, whereas neurotrophin-3 (NT3; EC_{50}, 1.7 ± 0.7 nM) behaved as a low-efficacy partial agonist with a maximum efficacy of 16 ± 4%. Nerve growth factor (NGF) as a negative control was inactive in this assay. Previously reported EC_{50} values are 0.7 nM for BDNF, 4 nM for NT4, and 1.3 nM for NT3 (*38*, *39*), consistent with our results.

Zinc ions, administered as zinc pyrithione (ZPT), induced TrkB phosphorylation with efficacy similar to that of BDNF (Fig. 2B) as was shown previously (*40*). However, ZPT-induced TrkB phosphorylation was not inhibited by the established TrkB inhibitor K252a (Fig. 2C) (*41*). These results are consistent with a TrkB transactivation mechanism through Zn^{2+}-mediated activation of the proto-oncogene tyrosine-protein kinase SRC (*42*). BDNF-induced activation was inhibited by K252a with a half maximal inhibitory concentration (IC_{50}) of 6 ± 4 nM (Fig. 2C), consistent with the previously reported value (IC_{50}, 3 nM) (*41*).

We applied this assay in additional cell lines; for example, human embryonic kidney (HEK) cells stably transfected with human TrkB (HEK-TrkB cells) displayed a signal-to-background (S/B) ratio of 10 to 20 (fig. S2), whereas cortical neuron cultures exhibited an S/B ratio of 2 to 5 (table S1). These assays were further validated using the compound DMAQ-B1, which produced weak phosphorylation of TrkB in HEK-TrkB cells (maximal efficacy, 16 ± 2%; fig. S3A), consistent with previously reported data (*29*). However, no DMAQ-B1–induced TrkB phosphorylation was detected in cortical neuron cultures.

(*30*). However, another study reported that although amitriptyline increased phosphorylation of TrkB in vivo, it did not simulate TrkB phosphorylation in vitro (*37*), implying that activation of TrkB by amitriptyline was induced indirectly. Deprenyl has also been reported to induce TrkB phosphorylation in vitro (*31*).

We set out to examine pharmacological parameters of these reported TrkB agonists in detail. To this end, we developed a battery of reliable, quantitative methods for direct measurement of phosphorylation of TrkB and downstream kinases in primary rat cortical neurons and in TrkB-transfected cells. We also used optical methods for TrkB activation and downstream gene activation in engineered living cells.

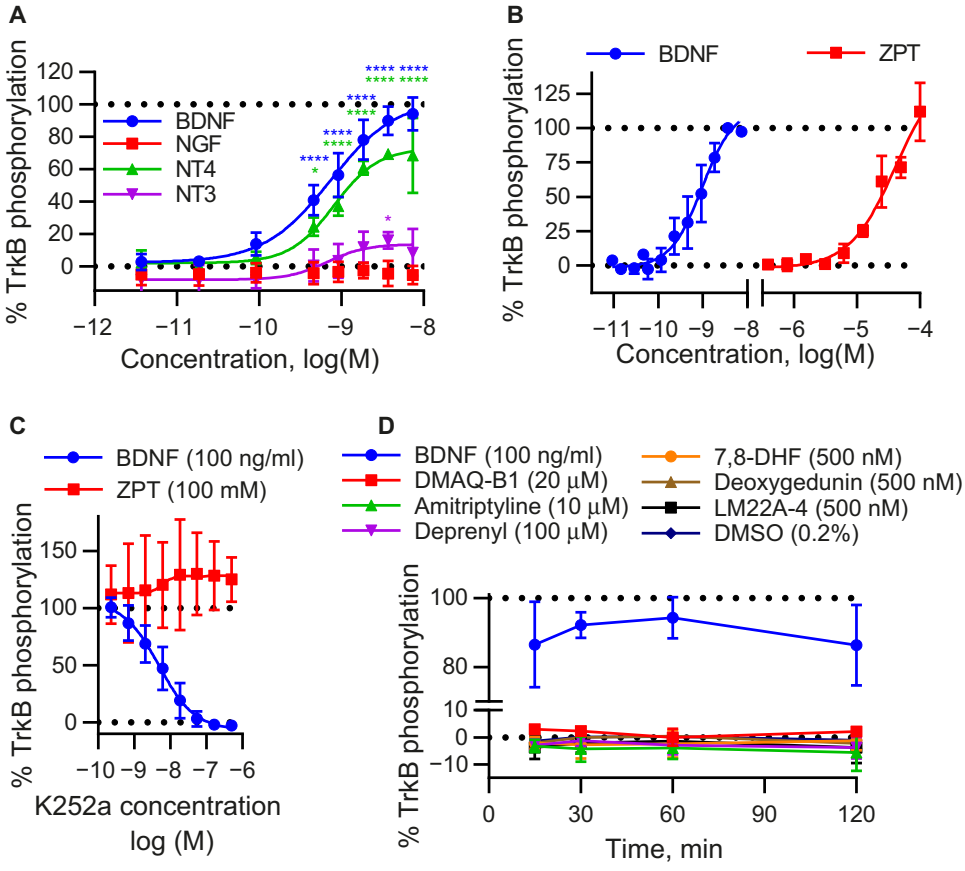

Fig. 2. Sandwich ELISA reliably measures the amount of TrkB phosphorylation in primary cortical neuron cultures. (**A**) Quantification of TrkB phosphorylation induced by BDNF, NT4, NT3, and NGF by sandwich ELISA. (**B**) Quantification of TrkB phosphorylation induced by ZPT (zinc pyrithione) by sandwich ELISA. (**C**) Effect of K252a on dose-dependent inhibition of BDNF-induced and ZPT-induced TrkB phosphorylation. (**D**) Quantification of TrkB phosphorylation in the presence of reported small-molecule TrkB agonists. The reported agonists were tested at the concentrations reported to elicit the greatest response. Data are normalized to BDNF maximal response and represent means ± SD of three independent experiments. Two-way analysis of variance (ANOVA) was used, followed by Dunnett's *t* test [compared to dimethyl sulfoxide (DMSO)]: **P* < 0.05, *****P* < 0.0001.

The results from our sandwich ELISAs were comparable to those from Western blot analysis using antibodies specific for phosphorylated TrkB (figs. S4 and S5). Thus, having established the validity of the sandwich ELISA using several known agonists and activators, we tested the reported small-molecule agonists of TrkB (Fig. 1G) over a range of different concentrations and treatment durations. However, we did not detect TrkB phosphorylation induced by 7,8-DHF, LM22A-4, deoxygedunin, amitriptyline, or deprenyl in cortical neurons (Fig. 2D), HEK-TrkB cells, or retinol-differentiated human neuroblastoma SH-SY5Y cells (figs. S3 to S6) under the conditions tested.

Direct measurement of downstream effector kinases AKT and ERK and their activation by enzyme-linked fixed-cell immunoassay

To detect signaling downstream of TrkB, we quantified phosphorylation (activation) of the serine-threonine protein kinase AKT and ERKs 1 and 2 (ERK1/2), both of which are activated downstream of TrkB (Fig. 1), in cortical neurons. We developed an enzyme-linked fixed-cell immunoassay (ELFI), wherein fixed cells are incubated with an antibody specific to the native, phosphorylated form of AKT or ERK1/2. The signal was detected through a chemiluminescent reaction of horseradish peroxidase (HRP) coupled to the secondary antibody and enhanced chemiluminescent (ECL) reagent. After detection, antibodies could be stripped off the cells, and a different set of primary antibody was applied. This approach allowed the detection of multiple target proteins in the same well. Although ELFI is highly dependent on antibody specificity, similar to Western blotting, the chemiluminescence readout provided reliable and reproducible results. S/B ratios of ELFI were ~2 to 4 for cortical neuron culture (table S1) and ~5 to 20 for cell lines with stable overexpression of TrkB (for example, HEK-TrkB; fig. S2).

BDNF and NT4 induced phosphorylation of AKT (Fig. 3A) and ERK (Fig. 3B) with similar efficacy and potency (table S2) in cortical neuron cultures. NT3 had lower efficacy in regard to stimulating AKT phosphorylation in cortical neuron cultures, which is consistent with the observed low efficacy of NT3 at stimulating TrkB phosphorylation (Fig. 3A); however, NT3 induced ERK activation to a degree similar to that induced by BDNF (Fig. 3B). The difference in efficacies of ERK and AKT activation could be due to low concentrations of the relevant adaptor proteins in the ERK pathway. Under such a scenario, a high amount of ERK activity may be induced by activation of a fraction of the available receptor pool, as shown previously (*43*). NGF had no effect on the basal amount of ERK and AKT phosphorylation, which indicates low abundance or absence of TrkA in cortical neuron cultures. When comparing activation of TrkB and downstream signaling proteins, BDNF had a greater (~10-fold) potency of activating ERK and AKT than at TrkB (Fig. 3C), consistent with amplification of the signaling events downstream of TrkB. Whereas low concentrations of K252a inhibited BDNF-induced activation of downstream effectors (fig. S7), higher concentrations of K252a inhibited activation of ERK in a manner that was independent of TrkB, thus providing only a narrow pharmacological window for TrkB-selective inhibition by this compound (fig. S7). ZPT activated ERK with similar efficacy and AKT with much greater efficacy in comparison to BDNF (Fig. 3D).

With the exception of DMAQ-B1, the reported small-molecule agonists did not induce AKT or ERK phosphorylation in cortical neuron culture at any time or concentration measured (Fig. 3E and figs. S3 and S6). DMAQ-B1 induced maximal AKT phosphorylation at 15 min with 20% efficacy, but AKT phosphorylation decayed rapidly, eventually resulting in lower abundance of phosphorylated AKT than under basal conditions. DMAQ-B1 induced maximal ERK phosphorylation at 15 min, as well, with 50% efficacy and showed a temporal profile similar to that of BDNF. Although we detected no DMAQ-B1–induced TrkB phosphorylation in cortical neuron culture, we detected

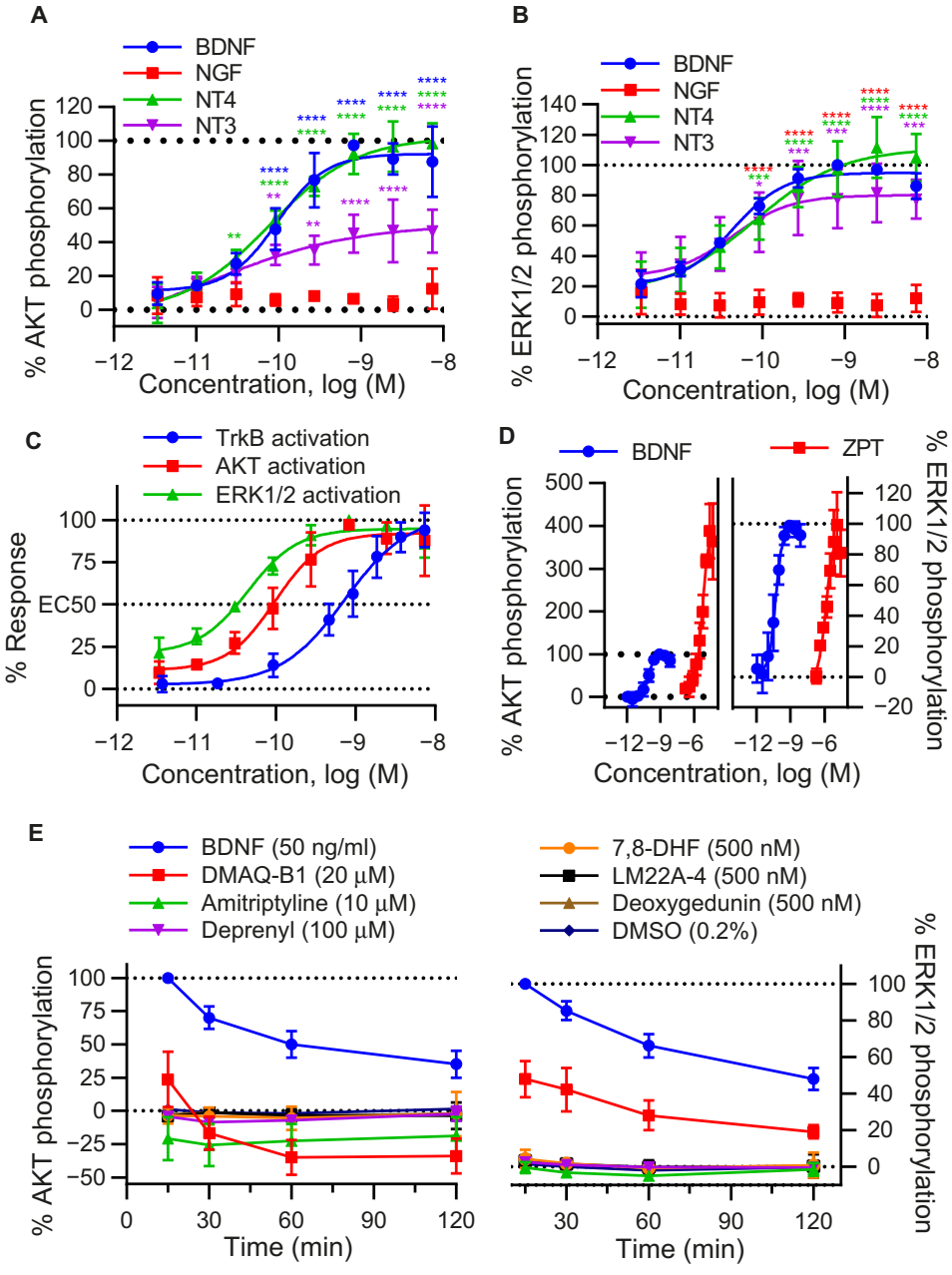

Fig. 3. ELFI reliably and quantitatively indicates the amount of ERK and AKT phosphorylation in primary cortical neuron cultures. (**A**) Quantification of AKT phosphorylation in response to treatment with BDNF, NT4, NT3, and NGF. (**B**) Quantification of ERK1/2 phosphorylation in response to treatment with BDNF, NT4, NT3, and NGF. (**C**) Phosphorylation of AKT, ERK1/2, and TrkB in response to BDNF treatment. (**D**) Phosphorylation of AKT and ERK1/2 in response to treatment with BDNF and ZPT. (**E**) Phosphorylation of AKT and ERK1/2 in response to reported small-molecule agonists of TrkB used at the indicated concentrations over a time course. Data are normalized to BDNF maximal response and represent means ± SD of three independent experiments. Two-way ANOVA was used, followed by Dunnett's *t* test (compared to DMSO): **P* < 0.05, ***P* < 0.01, ****P* < 0.001, *****P* < 0.0001.

a small amount of TrkB phosphorylation in HEK-TrkB cells (see previous section and fig. S3A). The mechanism of action of this compound remains unclear, however, owing to its toxicity and lack of selectivity. DMAQ-B1 has been reported to induce phosphorylation of all three Trk receptors as well as ERK and AKT. However, activation of ERK and AKT also occurred in the absence of Trk receptors. Furthermore, the compound exhibited significant toxicity at concentrations (≥20 μM) that induce Trk receptor phosphorylation (*29*). Regardless of the mechanism, which is likely complex and confounded by the toxicity, DMAQ-B1 provided additional validation of the assays described in this report by demonstrating the ability to detect low amounts of receptor and downstream kinase activation. Most notably, neither 7,8-DHF nor LM22A-4 induced dose-dependent AKT or ERK activation in cortical neuron culture (Fig. 3E and fig. S6). These results are in agreement with our TrkB activation experiments (sandwich ELISA data) and in contrast to previously reported data (*28*, *33*).

Failure of reported TrkB agonists to activate TrkB in cell assays

The S/B ratio of TrkB activation in cortical neurons was 2 to 5 (table S1), and the lowest statistically significant activation level detected was 16 ± 4% of maximal BDNF response, which represents a fivefold lower signal as illustrated by NT3 (Fig. 2A). In addition, low concentrations of DMAQ-B1 that elicited undetectable amounts of TrkB activation (<15%) induced 25 to 50% activation of ERK and AKT in cortical neuron culture, which was statistically significant in our assays (Fig. 3E). Moreover, the engineered cells stably expressing TrkB provided statistically significant signal at 5 to 10% of maximal BDNF response at TrkB (fig. S2). In addition to testing 7,8-DHF and LM22A-4 at reported concentrations, we also performed dose-response experiments at different time points to ensure that we did not miss any activity owing to potential experimental differences or deviations from standard dose-response curves. The results were the same as those described above: No significant activity was detected (fig. S6). Thus, given the number of different assays used and their detection sensitivity range established in this study, low-activity (meaning low efficacy) compounds would have been reliably detected in our assays (*33*).

High-throughput screen for small-molecule agonists and modulators

On the basis of these negative results, we decided to perform a pilot high-throughput screen (HTS) using a small-molecule library in search of compounds that reliably acted as TrkB agonists or allosteric modulators. We used the commercially available DiscoverX U2OS cell

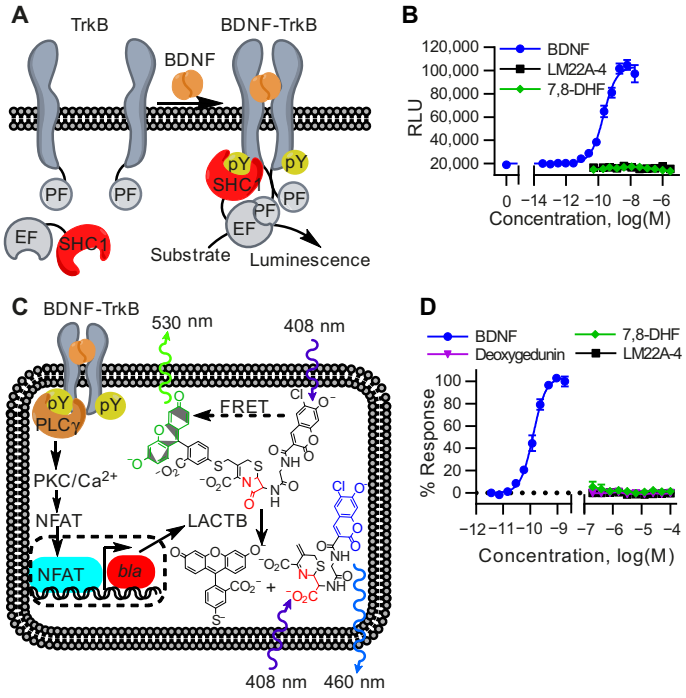

Fig. 4. Schematic representation of TrkB-dependent signal generation in engineered cells. (**A**) The DiscoverX PathHunter assay is based on U2OS cells transfected with the TrkB and SHC1 proteins, each fused with complementary fragments of the enzyme β-galactosidase. When brought together, the fragments reconstitute enzymatic activity and cleave the substrate to generate a luminescent product. To measure the ability of TrkB to recruit SHC1, which depends on TrkB phosphorylation, TrkB was fused to a peptide fragment (PF) and SHC1 to an enzyme fragment (EF). (**B**) Luminescence in relative light units (RLU) in the PathHunter assay when cells were treated with BDNF, LM22A-4, and 7,8-DHF. (**C**) NFAT-bla-TrkB-CHO CellSensor assay reports on TrkB activation through the expression of the β-lactamase (LACTB)–encoding gene *BLA* under the control of PLCγ-PKC-NFAT signaling. TrkB phosphorylation results in PLCγ activation, leading to an increase in Ca^{2+} concentration and subsequent NFAT activation (*65*), which controls production of β-lactamase in these cells. β-Lactamase in turn separates the coumarin and fluorescein derivative FRET (fluorescence resonance energy transfer) partners linked by the β-lactam system. (**D**) β-Lactamase activity in the CellSensor assay induced by BDNF, LM22A-4, and 7,8-DHF. Data are normalized to BDNF maximal response and represent means ± SD of a representative experiment.

line and PathHunter assay for this purpose (Fig. 4A). The assay reports on activation of TrkB through reconstitution of β-galactosidase activity in U2OS cells. Using ELFI for BDNF-induced ERK phosphorylation, we confirmed TrkB activity and ERK signaling in these cells (fig. S2F). BDNF induced a robust signal in the PathHunter assay with an S/B ratio of 4 to 6 and a Z′-factor, a screening window coefficient that assesses assay quality (*44*), equal to 0.6 (on a 384-well plate format), which is generally acceptable for high-throughput screening (an assay with Z′ equal or greater than 0.5 is considered to be suitable for HTS) (Fig. 4B). The reported small-molecule agonists (for example, 7,8-DHF and LM22A-4) did not evoke any response in this assay (Fig. 4B), confirming our previous ELISA results.

We also measured the consequences of TrkB activation on gene expression. We used the CellSensor assay as a counterscreen to the PathHunter assay. This assay is based on β-lactamase expression under the control of nuclear factor of activated T cells (NFAT) in a Chinese hamster ovary (CHO) cell line (Fig. 4C). BDNF induced β-lactamase expression with an S/B ratio of 5 to 8 and a Z′-factor of ≥0.9, which was feasible for high-throughput screening (Fig. 4D). This response was inhibited by K252a (fig. S8). TrkB expression and activation were confirmed in these cells with ELISA as described above (fig. S2, A to C). The reported small-molecule agonists failed to activate TrkB in this assay as well (Fig. 4D).

To identify possible agonists or modulators of BDNF-induced TrkB activation, we performed a primary screen of 40,000 compounds in the Broad Institute's central nervous system (CNS) diversity-oriented synthesis (DOS) library. This DOS library contains compounds that exhibit CNS-compatible drug-like properties, which were selected using in silico analysis and in vitro, cellular, and in vivo assays and models (*45*). We tested each compound for the ability to increase TrkB activation in the presence of BDNF at EC_{15} using the DiscoverX PathHunter cell system in a 384-well format, searching for both TrkB agonists and positive allosteric modulators. The primary screen identified 355 compounds as potential hits on the basis of activation three times above the SD of BDNF at EC_{15}. We used a counterscreen in TrkB-null DiscoverX PathHunter assay to eliminate false positives, thus shortening the list of candidate compounds to 83. Each of these 83 compounds was tested in the rest of our assays. The CellSensor assay identified only three compounds as potential positive allosteric modulators. However, none of these hits were confirmed to activate TrkB in cortical neurons using ELISA and ELFI (fig. S3F). As a result, high-throughput screening failed to identify any reliable lead compound from this library.

DISCUSSION

We were unable to confirm previous claims that the reported small-molecule agonists of TrkB activate this receptor in cell assays. The reported compounds showed no reliable activation of TrkB as measured by an extensive series of cellular assays that include rat and human receptors, expressed either natively or overexpressed in established cell lines. Multiple researchers at two different institutions (the Columbia and Broad groups) showed no reliable dose-dependent activation of the TrkB signaling system by these compounds, including the examination of TrkB phosphorylation, downstream kinase signaling, and gene expression. A report by the authors who introduced 7,8-DHF as a TrkB agonist has suggested that its activity in primary cortical neuron cultures is dependent on the number of days in vitro (DIV) of the cultures and reported significant activation of the receptor beyond DIV 15 (*33*). Preparing 7,8-DHF stock solution in DMSO immediately before the experiments was also carried out to eliminate any possibility of compound decomposition. However, adjusting our protocols to account for these possible sources of variability did not alter the outcome of our experiments. Although the difficulty of reproducing the reported in vitro results has been discussed at conferences for years, it is only recently that an independent research group has reported studies that failed to confirm some of the reported small-molecule compounds as TrkB agonists (7,8-DHF, LM22A-4, amitriptyline, and *N*-acetyl serotonin) (*46*). Our study reports on additional putative TrkB agonists and provides a detailed characterization of signaling downstream of TrkB in neurons treated with these compounds.

We propose that one plausible explanation for the observed discrepancies is methodological in nature. Although Western blotting is a standard core method in life sciences research, it requires many procedural steps, making it impractical to perform multiple repeats for each experimental condition plus controls (*47*–*49*). Moreover, densitometry is dependent on the analysis procedure, which may lead to biased results, especially with a low amount of phosphorylation of the protein of interest (*50*). Specificity of the antibody plays an important

role as well (*50*, *51*). Although antibodies recognizing phosphorylated ERK and phosphorylated AKT yielded highly specific staining on blots (fig. S5), we did not find an antibody that was specific for phosphorylated TrkB; the commercially available antibodies tended to recognize additional targets. Complementary methods should be applied to confirm Western blot results. In our view, the described quantitative ELISA provides sufficient throughput for controls and repeats to be used along with the blot to more accurately characterize drug activity. We recommend that Western blot be used as a qualitative or semiquantitative complementary method to the quantitative ELISA assays, as confirmation that ELISA indeed detects the desired phosphorylation reaction. Alternative methods that are independent of antibodies should also be considered, such as methods based on enzymatic activity of reporter proteins as the readout.

7,8-DHF has been tested in vivo in many different disease models by several independent laboratories. For example, systemic administration of 7,8-DHF to mice has been shown to have antidepressant effects (*52*), prevent memory loss in an Alzheimer's disease model (*53*), and improve motor function in Huntington's disease models (*54*). The behavioral or physiological outcomes reported in these studies are generally consistent with what would be expected for a TrkB agonist: inducing plasticity and enhancing repair. However, most of the in vivo reports of the molecular mechanism are based on Western blotting of postmortem animal samples. Given the drawbacks of immunoblotting, alternative, more robust assays should be used to directly confirm a TrkB-mediated mechanism of action.

In methodological terms, a key problem is that in vitro assays that afford the necessary probing power to characterize the mechanism of action of compounds at the molecular level (in this case, induction of TrkB receptor phosphorylation) are not readily applicable in vivo. In mechanistic terms, the in vitro experimental system may not represent the native in vivo receptor complex or recapitulate the possibilities of circuit-level effects, or both. For example, 7,8-DHF may indirectly activate TrkB in vivo through mechanisms that are simply not available in vitro. Pharmacokinetics may also play a role in the activity of the compound. 7,8-DHF is likely converted in the body into various metabolites that could induce the observed effects in vivo (*52*). It is also known that TrkB can undergo transactivation through the activation of several G protein (guanine nucleotide–binding protein)–coupled receptors or receptor tyrosine kinases, for example, epidermal growth factor receptor and SRC (*40*, *42*, *55*, *56*). Therefore, 7,8-DHF or its metabolite(s), or both, may also in theory induce transactivation of TrkB through other pathways that are not present in vitro. Several studies have reported TrkB-independent neuroprotective effects of 7,8-DHF in in vitro cell models and attributed these to its antioxidant properties (*57*, *58*). Although the in vivo activity of a compound is ultimately what matters for drugs and molecular probes, in vitro assays are an important tool typically required for detailed characterization and development of compound leads (*59*).

We conclude that the development of reliable TrkB agonists and activators with robust activity that translates between in vivo and in vitro systems remains a standing and important challenge. Therefore, previous data acquired with the reported compounds ought to be reinterpreted in light of our results.

MATERIALS AND METHODS

Chemical reagents and antibodies

Chemicals were purchased from different commercial sources: 7,8-DHF from TCI America; LM22A-2 and LM22A-3 from eMolecules; amitriptyline hydrochloride, deprenyl, and zinc with 2 equivalents of pyrithione ionophore (Zn-2PT; ZPT) from Sigma-Aldrich; L-783,281 (DMAQ-B1) and K252a from Tocris; and thapsigargin from Cayman Chemical. Deoxygedunin was synthesized from gedunin (Tocris) (*60*). LM22A-4 was synthesized in-house (see protocol). A list of antibodies is presented in table S3.

Cell lines

A HEK cell line stably transfected with human TrkB was a gift from M. V. Chao (New York University). Cells were cultured in a 5% CO_2 atmosphere at 37°C in Dulbecco's modified Eagle's medium (DMEM) with GlutaMAX (Life Technologies) supplemented with 10% fetal bovine serum (FBS) (Premium Select, Atlanta Biologicals), penicillin (100 U/ml) and streptomycin (100 μg/ml) (Life Technologies), and G418 sulfate (200 μg/ml) (MP Biomedicals).

SH-SY5Y cells were cultured in DMEM and Nutrient Mixture F-12 (HAM) [DMEM/F-12 (1:1)] (Life Technologies) supplemented with 10% FBS (Premium Select, Atlanta Biologicals), penicillin (100 U/ml), and streptomycin (100 μg/ml) (Life Technologies). To perform the experiments, cells were seeded in 24-well plates (2×10^5 cells per well) and incubated for 48 hours, and then the cells were washed with phosphate-buffered saline (PBS) and incubated for 48 hours in DMEM/F12 (1:1) supplemented with 4% FBS, penicillin (100 U/ml), streptomycin (100 μg/ml), and 10 μM all-trans-retinoic acid (Sigma). Before treatment with compounds, cells were incubated for at least 6 hours in medium without all-trans-retinoic acid.

Primary cortical neuron culture

Cortical neuron tissue from E18 (embryonic day 18) rat embryos were provided by the laboratory of C. Waites (Columbia University Medical Center, Department of Pathology and Cell Biology). Tissues were digested in TrypLE Express Enzyme (Gibco) for 15 to 30 min at 37°C, transferred to Neurobasal medium supplemented with B27 supplement (Life Technologies) and GlutaMAX (Life Technologies), triturated, counted in the presence of trypan blue (Sigma), and seeded on white flat-bottom 96-well plates (4×10^4 cells per well) or 12-well plates (2×10^5 to 3×10^5 cells per well) coated with poly-D-lysine (P6407, Sigma) and cultured in Neurobasal medium supplemented with B27 supplement without changing the medium until the experiment day.

Western blotting

On the day of the experiment, cells were washed and incubated with culturing medium without proteins (FBS or B-27 supplement) for 0.5 to 1 hour. Compounds at 5× of working concentrations were delivered in medium with ≤2.5% DMSO (to accommodate ≤0.5% DMSO in culture). Cells were treated for various time points as indicated. Experiments were stopped by removing the medium on ice, and cells were lysed with 100 μl of 2× loading buffer [20% glycerol, 125.2 mM tris, 4% SDS, 5% β-mercaptoethanol, bromophenol for color (pH 6.8) with 1:100 protease inhibitor cocktail, phosphatase inhibitor 2 and 3 cocktails (P5726 and P0044, Sigma), and 0.5 M EDTA solution or ELISA lysis buffer] and incubated over ice for 15 min to 1 hour, after which time cells were scraped and the lysates were transferred into microcentrifuge tubes. The tubes were centrifuged at 14,500 rpm for 10 min; the supernatant was transferred to fresh tubes, and the protein content was measured using the Pierce BCA (bicinchoninic acid) assay. Equal quantities of protein (typically 10 μg per lane) were added to each well of a 10% bis-tris acrylamide gel and were blotted onto Immobilon-P polyvinylidene difluoride transfer membranes. Blots were blocked in 3% bovine serum albumin (BSA) in tris-buffered saline for at least

30 min, followed by 1-hour incubation with the primary antibody with rocking at room temperature (RT). The blots were washed 3 × 5 min with tris-buffered saline plus Tween 20 (0.05%), incubated for 30 min with secondary antibody (typically 1:1000) in the buffer indicated on the antibody's corresponding data sheet, and then washed again for 3 × 5 min before development with the ECL kit (PI34079, Thermo Scientific). Chemiluminescence and light absorbance (for protein ladder) were visualized with a Kodak Image Station 440CF imager. Membranes were stripped and reprobed with the stripping buffer used in the in-cell ELISA, followed by the same detection procedure for the next target protein. The chemiluminescent image was overlaid to the absorbance image for representation.

Sandwich ELISA

The amount of TrkB phosphorylation was quantified using the previously described kinase receptor activation–ELISA (*61*) with slight modification. On the day of the experiment, cells were washed and incubated with culturing medium without proteins (FBS or B-27 supplement) for 0.5 to 1 hour. Compounds at 5× of working concentrations were delivered in medium with ≤2.5% DMSO (to accommodate ≤0.5% DMSO in culture). Cells were treated for various time points. For neurotrophic factor dose curves, 1-hour treatment was chosen because this time point provided the highest BDNF response. Experiments were stopped by removing the medium on ice, and cells were lysed in 100 μl of ELISA lysis buffer [0.15 M NaCl, 10 mM Trizma, 10 mM tris base, 2 mM EDTA, 1% Triton X-100, 10% glycerol (pH 8.0), 1:100 phosphatase inhibitor cocktail 2 (Sigma-Aldrich), and 1:100 protease inhibitor cocktail (Sigma-Aldrich)]. Experimental plates were kept at −20°C (or −80°C for a long-term storage) until transfer to an ELISA plate (NUNC Immulon 4 HBX) that was coated overnight at 4°C with an appropriate TrkB-capturing antibody [PBS; rabbit polyclonal antibody (0.8 μg/ml) recognizing TrkB (10047-RP02, Sino Biologicals) or goat polyclonal antibody (1 μg/ml) recognizing TrkB (T1941, Sigma-Aldrich) for phosphorylation assays, or goat polyclonal antibody (1 μg/ml) recognizing TrkB (AF397, R&D Systems) for total TrkB assays] for 2 to 3 hours at RT or overnight at 4°C. ELISA plates were washed five times with 150 μl of washing buffer (PBS, 0.05% Tween 20) and blocked (PBS, 1% BSA) for 1 hour at RT before transfer of 80 and 20 μl of lysate for phosphorylation and total TrkB assays, respectively, for overnight incubation at 4°C. On the next day, ELISA plates were washed and incubated with an appropriate detecting antibody. Tyrosine phosphorylation was quantified by 1-hour incubation with HRP-conjugated monoclonal antibody recognizing phosphorylated Tyr (1:2500; #HAM1676, R&D Systems) in washing buffer with 0.1% BSA, followed by 30-min color development of TMB One Solution (Promega). The plates were then quenched with 1 N HCl, and the absorbance was measured at 450 nm on Synergy H1 plate reader (BioTek Instruments Inc.). Total TrkB was quantified similarly using an antibody against TrkB antibody (0.8 μg/ml; 1.5-hour incubation; #10047-RP02, Sino Biologicals) and HRP-conjugated antibody against rabbit immunoglobulin G (1:1000; Cell Signaling Technologies).

Enzyme-linked fixed-cell immunoassay

The amount of phosphorylation of downstream signaling proteins was quantified using ELFI. Cells were treated similarly to sandwich ELISA. Experiments were stopped by fixing the cells in 4% formaldehyde (Sigma) for 20 min. Cells were permeabilized with washing buffer, blocked in washing buffer with 10% BSA, and incubated with detecting antibody for the protein of interest for 2 hours at RT or overnight at 4°C. Appropriate HRP-linked secondary antibody was applied, and luminescence (SuperSignal ELISA Pico Chemiluminescent Substrate, Thermo Scientific) was detected on the plate reader. To quantify different proteins in the same plate, antibodies were stripped using stripping buffer (*62*) [6 M guanidine·HCl, 0.2% Triton X-100, 20 mM tris·HCl (pH 7.5)] for 5 min, washed, blocked, and treated with another antibody. Stripping and reprobing cycles were done up to six times.

DiscoverX PathHunter assay

U2OS cells expressing both TrkB and p75 neurotrophin receptor (TrkB-p75NTR cells) were cultured according to the manufacturer's instructions. PathHunter U2OS TrkB-p75NTR cells were detached by detachment reagent (DiscoverX) and resuspended in Plating 16 reagent (DiscoverX). Cells (5000 cells per well) were plated in 384-well plates (Corning) using Multidrop Combi (Thermo Fisher). Plates were incubated at 37°C in 5% CO_2 for about 20 hours. Compounds were pin-transferred to the cells. For the agonist assay, cells with compounds were incubated for 3 hours at 37°C. For the allosteric agonist assay, cells were treated with compounds first and, after 3 min, BDNF at EC_{15} (DiscoverX) was added for 3 hours (incubation at 37°C). Detection reagent (DiscoverX) was added for incubation for 1 hour at RT in the dark. The luminescence was measured in the EnVision plate reader (PerkinElmer).

The CellSensor assay

Invitrogen CHO K1 cell line with a CellSensor construct (TrkB-NFAT-bla) was obtained from Life Technologies and cultured in growth medium (DMEM with GlutaMAX) supplemented with 10% dialyzed FBS (Invitrogen), 1× MEM NEAA (minimum essential medium non-essential amino acid) solution (Sigma), 25 mM Hepes (Sigma), blasticidin (5 μg/ml) (Life Technologies), and Zeocin (200 μg/ml) (Life Technologies). The assay was performed according to the Invitrogen protocol. Briefly, cells were seeded in 384-well plates at 1.2×10^4 cells per well in a medium without blasticidin and Zeocin overnight using Multidrop Combi (Thermo Fisher). On the next day, cells were treated with compounds for 5 hours. After treatment, wells were loaded with β-lactamase LiveBLAzer-FRET B/G substrate (CCF4-AM, K1095, Invitrogen) for 2 hours. Fluorescence at 450 and 510 nm was recorded on a plate reader (excitation wavelength, 410 nm).

High-throughput screen

The CNS DOS library is a set of 40,000 unique small-molecule compounds biased for drug-like properties in the CNS. The library was designed through a data-driven selection of chemical scaffolds with high likelihood of CNS drug-like properties based on in silico (partition coefficient, topological polar surface area), in vitro, cellular, and in vivo assays and models, such as solubility, permeability, and the psychoactive drug screening program panel (*45*). Following these design principles, we evaluated the use of these scaffolds for the generation of lead-like molecules to be used in targeting the CNS and hoped to discover new and improved chemical matter against known but difficult targets such as TrkB. Primary screening was performed in the presence of BDNF at EC_{15} (allosteric mode), in duplicate at 20 μM single dose on DiscoverX U2OS TrkB-P75NTR cells using PathHunter assay. Compounds were delivered using CyBi-Well Vario (CyBio Biotechnology). The selection criterion was a signal 3× above the SD of the EC_{15} BDNF control. Primary screening identified 192 active compounds (duplicate wells 3× above the SD) and 163 inconclusive hits (one well 3× above the SD). These 355 compounds were retested for dose response (starting from 50 μM twofold serial dilution, 10 points,

duplicate plates) in allosteric and agonistic modes (in the absence of BDNF) in DRX U2OS TrkB-p75NTR cells using PathHunter assay. Compounds with a signal 3× above the SD at ≤20 μM were selected, resulting in 52 allosteric hits (active in allosteric mode) and 29 agonistic hits (active in agonistic mode, 23 overlapped with allosteric mode). These 58 compounds and 25 "cherry-picked" compounds based on their dose-response trends were counterscreened in two different DiscoverX U2OS cell lines (one expressing cholinergic receptor muscarinic 1 and β-Arrestin, the other expressing nuclear factor erythroid 2-related factor 2 and Kelch-like ECH-associated protein 1). Next, 83 compounds were counterscreened in CellSensor assay, sandwich ELISA in cortical neuron culture, and sandwich ELISA and ELFI in HEK-TrkB for dose response (four or eight concentrations with two separate serial dilutions: four-point 5× dilution starting from 50 μM and eight-point 2× dilution starting from 30 μM) in allosteric and agonistic modes. None of the compounds were found to be active at TrkB on the basis of the set statistical threshold.

Synthesis of deoxygedunin

Deoxygedunin was prepared from gedunin as described in the literature (*60*). Gedunin (7 mg, 14.5 μmol) was dissolved in degassed acetone (1.5 ml), and an excess of chromium(II) chloride was added at RT. The mixture was stirred for 8 days at RT, and the reaction progress was measured by high-performance liquid chromatography (HPLC) of small samples [methanol (MeOH)/phosphate buffer (pH 3 to 4) (80:20)]. Upon completion, the solvent was evaporated, and the crude material was diluted in water/dichloromethane (1:1) and then successively washed twice with brine and water, and each aqueous fraction was re-extracted with dichloromethane. The combined organic solvent was evaporated to dryness. The residual crude material was purified by preparative thin-layer chromatography [silica gel (500 μm)] in hexane/ethyl acetate (EtOAc) (1:1). The plate was scraped, and the collected product was desorbed from silica with EtOAc four times, evaporated, and dried under high vacuum for 2 days. The product was obtained as white powder (4 mg, 59% yield). ^{1}H nuclear magnetic resonance (NMR) (400 MHz; $CDCl_3$) peaks are as follows: δ 7.49 to 7.48 (m, 1H), 7.45 to 7.44 (m, 1H), 7.06 (d, J = 10.2 Hz, 1H), 6.43 (s, 1H), 5.88 (d, J = 10.2 Hz, 1H), 5.70 (s, 1H), 5.26 (t, J = 2.8 Hz, 1H), 4.99 (s, 1H), and 2.29 to 1.09 (not integrated) [consistent with literature data (*63*)]; mass spectrometry (atmospheric pressure chemical ionization) value calculated for $C_{28}H_{34}O_6$ is as follows: $[M]^+$, 466.24; identified values are as follows: $[M + H]^+$, 467.50; and $[M + MeOH + H]^+$, 499.50. Reversed-phase HPLC [MeOH/phosphate buffer (pH 3 to 4) (80:20)] was performed under the following conditions: RT, 33.3 min; maximum absorbance, 228 nm; Max Plot purity (220 to 800 nm), 93%.

Synthesis of LM22A-4

A solution of 1,3,5-benzenetricarbonyl trichloride (1.0 g, 3.8 mmol) in anhydrous dichloromethane (10 ml) was added dropwise to ethanolamine (2.3 ml, 38 mmol) at RT. After 30 min, the reaction was diluted with water (10 ml) and extracted with chloroform/isopropanol (1:1) (3 × 30 ml). The combined organics were dried over $MgSO_4$ and concentrated to a crude yellow solid. This crude material was then recrystallized in MeOH/dichloromethane and hexanes to give the pure product as fine white powder (600 mg, 47% yield). ^{1}H NMR (400 MHz, methanol-d4) peaks are as follows: δ 8.45 (s, 3H), 3.78 (t, J = 5.8 Hz, 6H), and 3.57 (t, J = 5.7 Hz, 6H). ^{13}C NMR (101 MHz, methanol-d4) peaks are as follows: δ 168.83, 136.53, 129.92, 61.50, and 43.68.

Statistical analysis

Statistical analysis was performed using GraphPad Prism software via two-way ANOVA analysis, followed by Dunnett's t test (compared to DMSO). Statistical significance was assigned by stars: *P < 0.05, **P < 0.01, ***P < 0.001, and ****P < 0.0001. Dose-response curves were fit using the GraphPad built-in nonlinear function log[agonists] versus response with variable slope and four parameters. S/B ratios were calculated by dividing the highest positive response value by the negative control value (typically DMSO).

SUPPLEMENTARY MATERIALS

www.sciencesignaling.org/cgi/content/full/10/493/eaal1670/DC1
Fig. S1. Antibody screen for sandwich ELISA.
Fig. S2. Characterization of assays in TrkB-expressing cells.
Fig. S3. Characterization of reported agonists in TrkB-expressing cells and HTS results.
Fig. S4. Western blot analysis of reported agonists in HEK-TrkB cells.
Fig. S5. Western blot analysis of reported agonists in cortical neuron culture.
Fig. S6. Activity of 7,8-DHF and LM22A-4 in cortical neuron culture under different conditions.
Fig. S7. K252a inhibition of ERK1/2 in cortical neuron culture.
Fig. S8. K252a inhibition in CellSensor assay.
Table S1. S/B values of ELISA and ELFI in cortical neuron culture.
Table S2. EC_{50} values of neurotrophic factors.
Table S3. List of antibodies used in this study.
Reference (*66*)

REFERENCES AND NOTES

1. L. Minichiello, TrkB signalling pathways in LTP and learning. *Nat. Rev. Neurosci.* **10**, 850–860 (2009).
2. A. Yoshii, M. Constantine-Paton, Postsynaptic BDNF-TrkB signaling in synapse maturation, plasticity, and disease. *Dev. Neurobiol.* **70**, 304–322 (2010).
3. P. Bekinschtein, M. Cammarota, J. H. Medina, BDNF and memory processing. *Neuropharmacology* **76** (Pt. C), 677–683 (2014).
4. I. Ninan, Synaptic regulation of affective behaviors; role of BDNF. *Neuropharmacology* **76** (Pt. C), 684–695 (2014).
5. B. Lu, G. Nagappan, Y. Lu, BDNF and synaptic plasticity, cognitive function, and dysfunction. *Handb. Exp. Pharmacol.* **220**, 223–250 (2014).
6. J. F. Maya Vetencourt, A. Sale, A. Viegi, L. Baroncelli, R. De Pasquale, O. F. O'Leary, E. Castrén, L. Maffei, The antidepressant fluoxetine restores plasticity in the adult visual cortex. *Science* **320**, 385–388 (2008).
7. J. A. Siuciak, D. R. Lewis, S. J. Wiegand, R. M. Lindsay, Antidepressant-like effect of brain-derived neurotrophic factor (BDNF). *Pharmacol. Biochem. Behav.* **56**, 131–137 (1997).
8. T. Saarelainen, P. Hendolin, G. Lucas, E. Koponen, M. Sairanen, E. MacDonald, K. Agerman, A. Haapasalo, H. Nawa, R. Aloyz, P. Ernfors, E. Castrén, Activation of the TrkB neurotrophin receptor is induced by antidepressant drugs and is required for antidepressant-induced behavioral effects. *J. Neurosci.* **23**, 349–357 (2003).
9. C. Pittenger, R. S. Duman, Stress, depression, and neuroplasticity: A convergence of mechanisms. *Neuropsychopharmacology* **33**, 88–109 (2008).
10. K. Martinowich, H. Manji, B. Lu, New insights into BDNF function in depression and anxiety. *Nat. Neurosci.* **10**, 1089–1093 (2007).
11. F. Boulle, G. Kenis, M. Cazorla, M. Hamon, H. W. M. Steinbusch, L. Lanfumey, D. L. A. van den Hove, TrkB inhibition as a therapeutic target for CNS-related disorders. *Prog. Neurobiol.* **98**, 197–206 (2012).
12. E. Castrén, Neurotrophins and psychiatric disorders. *Handb. Exp. Pharmacol.* **220**, 461–479 (2014).
13. K. Hashimoto, Brain-derived neurotrophic factor as a biomarker for mood disorders: An historical overview and future directions. *Psychiatry Clin. Neurosci.* **64**, 341–357 (2010).
14. E. Castrén, T. Rantamäki, The role of BDNF and its receptors in depression and antidepressant drug action: Reactivation of developmental plasticity. *Dev. Neurobiol.* **70**, 289–297 (2010).
15. T. Rantamäki, P. Hendolin, A. Kankaanpää, J. Mijatovic, P. Piepponen, E. Domenici, M. V. Chao, P. T. Männistö, E. Castrén, Pharmacologically diverse antidepressants rapidly activate brain-derived neurotrophic factor receptor TrkB and induce phospholipase-Cγ signaling pathways in mouse brain. *Neuropsychopharmacology* **32**, 2152–2162 (2007).

16. Y. Li, B. W. Luikart, S. Birnbaum, J. Chen, C.-H. Kwon, S. G. Kernie, R. Bassel-Duby, L. F. Parada, TrkB regulates hippocampal neurogenesis and governs sensitivity to antidepressive treatment. *Neuron* **59**, 399–412 (2008).
17. M. Bergami, R. Rimondini, S. Santi, R. Blum, M. Götz, M. Canossa, Deletion of TrkB in adult progenitors alters newborn neuron integration into hippocampal circuits and increases anxiety-like behavior. *Proc. Natl. Acad. Sci. U.S.A.* **105**, 15570–15575 (2008).
18. R. S. Duman, N. Li, R.-J. Liu, V. Duric, G. Aghajanian, Signaling pathways underlying the rapid antidepressant actions of ketamine. *Neuropharmacology* **62**, 35–41 (2012).
19. B. Lu, G. Nagappan, X. Guan, P. J. Nathan, P. Wren, BDNF-based synaptic repair as a disease-modifying strategy for neurodegenerative diseases. *Nat. Rev. Neurosci.* **14**, 401–416 (2013).
20. V. K. Gupta, Y. You, V. B. Gupta, A. Klistorner, S. L. Graham, TrkB receptor signalling: Implications in neurodegenerative, psychiatric and proliferative disorders. *Int. J. Mol. Sci.* **14**, 10122–10142 (2013).
21. C. Zuccato, E. Cattaneo, Huntington's disease. *Handb. Exp. Pharmacol.* **220**, 357–409 (2014).
22. C. Hock, K. Heese, C. Hulette, C. Rosenberg, U. Otten, Region-specific neurotrophin imbalances in Alzheimer disease: Decreased levels of brain-derived neurotrophic factor and increased levels of nerve growth factor in hippocampus and cortical areas. *Arch. Neurol.* **57**, 846–851 (2000).
23. A. Jerónimo-Santos, S. H. Vaz, S. Parreira, S. Rapaz-Lérias, A. P. Caetano, V. Buée-Scherrer, E. Castrén, C. A. Valente, D. Blum, A. M. Sebastião, M. J. Diógenes, Dysregulation of TrkB receptors and BDNF function by amyloid-β peptide is mediated by calpain. *Cereb. Cortex* **25**, 3107–3121 (2015).
24. A. Machado Dias, Bioinformatics approach to BDNF and BDNF-related disorders. *Curr. Neuropharmacol.* **9**, 318–329 (2011).
25. F. M. Longo, S. M. Massa, Small-molecule modulation of neurotrophin receptors: A strategy for the treatment of neurological disease. *Nat. Rev. Drug Discov.* **12**, 507–525 (2013).
26. S.-W. Jang, X. Liu, M. Yepes, K. R. Shepherd, G. W. Miller, Y. Liu, W. D. Wilson, G. Xiao, B. Blanchi, Y. E. Sun, K. Ye, A selective TrkB agonist with potent neurotrophic activities by 7,8-dihydroxyflavone. *Proc. Natl. Acad. Sci. U.S.A.* **107**, 2687–2692 (2010).
27. S.-W. Jang, X. Liu, C. B. Chan, S. A. France, I. Sayeed, W. Tang, X. Lin, G. Xiao, R. Andero, Q. Chang, K. J. Ressler, K. Ye, Deoxygedunin, a natural product with potent neurotrophic activity in mice. *PLOS ONE* **5**, e11528 (2010).
28. S. M. Massa, T. Yang, Y. Xie, J. Shi, M. Bilgen, J. N. Joyce, D. Nehama, J. Rajadas, F. M. Longo, Small molecule BDNF mimetics activate TrkB signaling and prevent neuronal degeneration in rodents. *J. Clin. Invest.* **120**, 1774–1785 (2010).
29. N. Wilkie, P. B. Wingrove, J. G. Bilsland, L. Young, S. J. Harper, F. Hefti, S. Ellis, S. J. Pollack, The non-peptidyl fungal metabolite L-783,281 activates TRK neurotrophin receptors. *J. Neurochem.* **78**, 1135–1145 (2001).
30. S.-W. Jang, X. Liu, C.-B. Chan, D. Weinshenker, R. A. Hall, G. Xiao, K. Ye, Amitriptyline is a TrkA and TrkB receptor agonist that promotes TrkA/TrkB heterodimerization and has potent neurotrophic activity. *Chem. Biol.* **16**, 644–656 (2009).
31. K. Nakaso, C. Nakamura, H. Sato, K. Imamura, T. Takeshima, K. Nakashima, Novel cytoprotective mechanism of anti-parkinsonian drug deprenyl: PI3K and Nrf2-derived induction of antioxidative proteins. *Biochem. Biophys. Res. Commun.* **339**, 915–922 (2006).
32. B. Zhang, G. Salituro, D. Szalkowski, Z. Li, Y. Zhang, I. Royo, D. Vilella, M. T. Díez, F. Pelaez, C. Ruby, R. L. Kendall, X. Mao, P. Griffin, J. Calaycay, J. R. Zierath, J. V. Heck, R. G. Smith, D. E. Moller, Discovery of a small molecule insulin mimetic with antidiabetic activity in mice. *Science* **284**, 974–977 (1999).
33. X. Liu, O. Obianyo, C. B. Chan, J. Huang, S. Xue, J. J. Yang, F. Zeng, M. Goodman, K. Ye, Biochemical and biophysical investigation of the brain-derived neurotrophic factor mimetic 7,8-dihydroxyflavone in the binding and activation of the TrkB receptor. *J. Biol. Chem.* **289**, 27571–27584 (2014).
34. A. W. English, K. Liu, J. M. Nicolini, A. M. Mulligan, K. Ye, Small-molecule trkB agonists promote axon regeneration in cut peripheral nerves. *Proc. Natl. Acad. Sci. U.S.A.* **110**, 16217–16222 (2013).
35. D. A. Schmid, T. Yang, M. Ogier, I. Adams, Y. Mirakhur, Q. Wang, S. M. Massa, F. M. Longo, D. M. Katz, A TrkB small molecule partial agonist rescues TrkB phosphorylation deficits and improves respiratory function in a mouse model of Rett syndrome. *J. Neurosci.* **32**, 1803–1810 (2012).
36. D. A. Simmons, N. P. Belichenko, T. Yang, C. Condon, M. Monbureau, M. Shamloo, D. Jing, S. M. Massa, F. M. Longo, A small molecule TrkB ligand reduces motor impairment and neuropathology in R6/2 and BACHD mouse models of Huntington's disease. *J. Neurosci.* **33**, 18712–18727 (2013).
37. T. Rantamäki, L. Vesa, H. Antila, A. Di Lieto, P. Tammela, A. Schmitt, K.-P. Lesch, M. Rios, E. Castrén, Antidepressant drugs transactivate TrkB neurotrophin receptors in the adult rodent brain independently of BDNF and monoamine transporter blockade. *PLOS ONE* **6**, e20567 (2011).
38. M. D. Sadick, A. Galloway, D. Shelton, V. Hale, S. Weck, V. Anicetti, W. L. T. Wong, Analysis of neurotrophin/receptor interactions with a gD-flag-modified quantitative kinase receptor activation (gD.KIRA) enzyme-linked immunosorbent assay. *Exp. Cell Res.* **234**, 354–361 (1997).
39. H. Antila, H. Autio, L. Turunen, K. Harju, P. Tammela, K. Wennerberg, J. Yli-Kauhaluoma, H. J. Huttunen, E. Castrén, T. Rantamäki, Utilization of in situ ELISA method for examining Trk receptor phosphorylation in cultured cells. *J. Neurosci. Methods* **222**, 142–146 (2014).
40. Y. Z. Huang, E. Pan, Z.-Q. Xiong, J. O. McNamara, Zinc-mediated transactivation of TrkB potentiates the hippocampal mossy fiber-CA3 pyramid synapse. *Neuron* **57**, 546–558 (2008).
41. P. Tapley, F. Lamballe, M. Barbacid, K252a is a selective inhibitor of the tyrosine protein kinase activity of the trk family of oncogenes and neurotrophin receptors. *Oncogene* **7**, 371–381 (1992).
42. Y. Z. Huang, J. O. McNamara, Mutual regulation of Src family kinases and the neurotrophin receptor TrkB. *J. Biol. Chem.* **285**, 8207–8217 (2010).
43. T. Shi, M. Niepel, J. E. McDermott, Y. Gao, C. D. Nicora, W. B. Chrisler, L. M. Markillie, V. A. Petyuk, R. D. Smith, K. D. Rodland, P. K. Sorger, W.-J. Qian, H. S. Wiley, Conservation of protein abundance patterns reveals the regulatory architecture of the EGFR-MAPK pathway. *Sci. Signal.* **9**, rs6 (2016).
44. J.-H. Zhang, T. D. Y. Chung, K. R. Oldenburg, A simple statistical parameter for use in evaluation and validation of high throughput screening assays. *J. Biomol. Screen.* **4**, 67–73 (1999).
45. J. T. Lowe, M. D. Lee IV, L. B. Akella, E. Davoine, E. J. Donckele, L. Durak, J. R. Duvall, B. Gerard, E. B. Holson, A. Joliton, S. Kesavan, B. C. Lemercier, H. Liu, J.-C. Marié, C. A. Mulrooney, G. Muncipinto, M. Welzel-O'Shea, L. M. Panko, A. Rowley, B.-C. Suh, M. Thomas, F. F. Wagner, J. Wei, M. A. Foley, L. A. Marcaurelle, Synthesis and profiling of a diverse collection of azetidine-based scaffolds for the development of CNS-focused lead-like libraries. *J. Org. Chem.* **77**, 7187–7211 (2012).
46. D. Todd, I. Gowers, S. J. Dowler, M. D. Wall, G. McAllister, D. F. Fischer, S. Dijkstra, S. A. Fratantoni, R. van de Bospoort, J. Veenman-Koepke, G. Flynn, J. Arjomand, C. Dominguez, I. Munoz-Sanjuan, J. Wityak, J. A. Bard, A monoclonal antibody TrkB receptor agonist as a potential therapeutic for Huntington's disease. *PLOS ONE* **9**, e87923 (2014).
47. K. A. Janes, An analysis of critical factors for quantitative immunoblotting. *Sci. Signal.* **8**, rs2 (2015).
48. T. A. Gorr, J. Vogel, Western blotting revisited: Critical perusal of underappreciated technical issues. *Proteomics Clin. Appl.* **9**, 396–405 (2015).
49. J. J. Bass, D. J. Wilkinson, D. Rankin, B. E. Phillips, N. J. Szewczyk, K. Smith, P. J. Atherton, An overview of technical considerations for Western blotting applications to physiological research. *Scand. J. Med. Sci. Sports* **27**, 4–25 (2017).
50. M. Gassmann, B. Grenacher, B. Rohde, J. Vogel, Quantifying Western blots: Pitfalls of densitometry. *Electrophoresis* **30**, 1845–1855 (2009).
51. S. C. Taylor, T. Berkelman, G. Yadav, M. Hammond, A defined methodology for reliable quantification of Western blot data. *Mol. Biotechnol.* **55**, 217–226 (2013).
52. X. Liu, Q. Qi, G. Xiao, J. Li, H. R. Luo, K. Ye, *O*-methylated metabolite of 7,8-dihydroxyflavone activates TrkB receptor and displays antidepressant activity. *Pharmacology* **91**, 185–200 (2013).
53. Y. Zeng, Y. Liu, M. Wu, J. Liu, Q. Hu, Activation of TrkB by 7,8-dihydroxyflavone prevents fear memory defects and facilitates amygdalar synaptic plasticity in aging. *J. Alzheimers Dis.* **31**, 765–778 (2012).
54. M. Jiang, Q. Peng, X. Liu, J. Jin, Z. Hou, J. Zhang, S. Mori, C. A. Ross, K. Ye, W. Duan, Small-molecule TrKB receptor agonists improve motor function and extend survival in a mouse model of Huntington's disease. *Hum. Mol. Genet.* **22**, 2462–2470 (2013).
55. M. Domeniconi, M. V. Chao, Transactivation of Trk receptors in spinal motor neurons. *Histol. Histopathol.* **25**, 1207–1213 (2010).
56. D. Puehringer, N. Orel, P. Lüningschrör, N. Subramanian, T. Herrmann, M. V. Chao, M. Sendtner, EGF transactivation of Trk receptors regulates the migration of newborn cortical neurons. *Nat. Neurosci.* **16**, 407–415 (2013).
57. X. Han, S. Zhu, B. Wang, L. Chen, R. Li, W. Yao, Z. Qu, Antioxidant action of 7,8-dihydroxyflavone protects PC12 cells against 6-hydroxydopamine-induced cytotoxicity. *Neurochem. Int.* **64**, 18–23 (2014).
58. J. Chen, K.-W. Chua, C. C. Chua, H. Yu, A. Pei, B. H. L. Chua, R. C. Hamdy, X. Xu, C.-F. Liu, Antioxidant activity of 7,8-dihydroxyflavone provides neuroprotection against glutamate-induced toxicity. *Neurosci. Lett.* **499**, 181–185 (2011).
59. C. H. Arrowsmith, J. E. Audia, C. Austin, J. Baell, J. Bennett, J. Blagg, C. Bountra, P. E. Brennan, P. J. Brown, M. E. Bunnage, C. Buser-Doepner, R. M. Campbell, A. J. Carter, P. Cohen, R. A. Copeland, B. Cravatt, J. L. Dahlin, D. Dhanak, A. M. Edwards, M. Frederiksen, S. V. Frye, N. Gray, C. E. Grimshaw, D. Hepworth, T. Howe, K. V. M. Huber, J. Jin, S. Knapp, J. D. Kotz, R. G. Kruger, D. Lowe, M. M. Mader, B. Marsden, A. Mueller-Fahrnow, S. Müller, R. C. O'Hagan, J. P. Overington, D. R. Owen, S. H. Rosenberg, B. Roth, R. Ross, M. Schapira, S. L. Schreiber, B. Shoichet, M. Sundström, G. Superti-Furga, J. Taunton, L. Toledo-Sherman,

C. Walpole, M. A. Walters, T. M. Willson, P. Workman, R. N. Young, W. J. Zuercher, The promise and peril of chemical probes. *Nat. Chem. Biol.* **11**, 536–541 (2015).
60. A. R. H. Kehrli, D. A. H. Taylor, A synthesis of methyl 2α-acetoxy-3-deoxo-3α-hydroxyangolensate. *J. Chem. Soc. Perkin Trans. 1* **1990**, 2067–2070 (1990).
61. M. D. Sadick, A. Intintoli, V. Quarmby, A. McCoy, E. Canova-Davis, V. Ling, Kinase receptor activation (KIRA): A rapid and accurate alternative to end-point bioassays. *J. Pharm. Biomed. Anal.* **19**, 883–891 (1999).
62. Y.-G. Yeung, E. R. Stanley, A solution for stripping antibodies from polyvinylidene fluoride immunoblots for multiple reprobing. *Anal. Biochem.* **389**, 89–91 (2009).
63. J. W. Powell, Nuclear magnetic resonance spectroscopy. A correlation of the spectra of some meliacins and their derivatives. *J. Chem. Soc. C* **1966**, 1794–1798 (1966).
64. E. J. Huang, L. F. Reichardt, Trk receptors: Roles in neuronal signal transduction. *Annu. Rev. Biochem.* **72**, 609–642 (2003).
65. J. Wang, M. K. Hancock, J. M. Dudek, K. Bi, Cellular assays for high-throughput screening for modulators of Trk receptor tyrosine kinases. *Curr. Chem. Genomics* **1**, 27–33 (2008).
66. D. R. Kaplan, K. Matsumoto, E. Lucarelli, C. J. Thiele, Induction of TrkB by retinoic acid mediates biologic responsiveness to BDNF and differentiation of human neuroblastoma cells. *Neuron* **11**, 321–331 (1993).

Acknowledgments: We thank M. V. Chao (New York University School of Medicine, Skirball Institute of Biomolecular Medicine) for providing PC12 cells and HEK cells stably transfected with TrkB. We would also like to thank C. Waites (Columbia University Medical Center, Department of Pathology and Cell Biology) for providing the rat cortical neurons and T. Zheng (Columbia University, Department of Statistics) for assistance with the statistical analysis. **Funding:** This study was supported by Columbia University and the Stanley Medical Research Institute of the Broad Institute of Massachusetts Institute of Technology and Harvard University. **Author contributions:** U.B., Y.M., and D.S. designed the project; U.B., Y.M., F.T., T.J., and M.G. performed the experiments; E.H., M.P., and Q.X. designed the HTS; Q.X., F.W., and Y.-L.Z. performed the HTS; U.B. and D.S. wrote the manuscript. **Competing interests:** The authors declare that they have no competing interests.

Submitted 6 October 2016
Resubmitted 5 April 2017
Accepted 24 July 2017
Published 22 August 2017
10.1126/scisignal.aal1670

Citation: U. Boltaev, Y. Meyer, F. Tolibzoda, T. Jacques, M. Gassaway, Q. Xu, F. Wagner, Y.-L. Zhang, M. Palmer, E. Holson, D. Sames, Multiplex quantitative assays indicate a need for re-evaluating reported small-molecule TrkB agonists. *Sci. Signal.* **10**, eaal1670 (2017).

Science Signaling

Multiplex quantitative assays indicate a need for reevaluating reported small-molecule TrkB agonists

Umed Boltaev, Yves Meyer, Farangis Tolibzoda, Teresa Jacques, Madalee Gassaway, Qihong Xu, Florence Wagner, Yan-Ling Zhang, Michelle Palmer, Edward Holson and Dalibor Sames

Sci. Signal. **10** (493), eaal1670.
DOI: 10.1126/scisignal.aal1670

Re-evaluating reported TrkB agonists

Activation of the receptor tropomyosin-related kinase B (TrkB) by brain-derived neurotrophic factor (BDNF) is important for neurodevelopment, memory, and cognition. Activation of TrkB is a potential therapeutic strategy for treating Alzheimer's disease and other brain disorders, but the pharmacokinetic properties of BDNF preclude using BDNF to activate TrkB in therapeutic contexts. Several small molecules have been reported to act as TrkB agonists and are widely used in disease models. Boltaev *et al*. developed a series of assays to quantitatively measure TrkB activation and downstream signaling events in cells treated with these reported BDNF agonists. The authors found that these compounds did not activate key aspects of TrkB signaling in contrast to BDNF or other neurotrophic factors that stimulate TrkB. These findings highlight the need for careful interpretation of the results of experiments using reported BDNF agonists.